Genotyping and data quality control in discovery cohorts

For SCES, a total of 1,952 venous blood-derived samples were genotyped using Illumina Human 610 Quad Beadchips (Illumina Inc., San Diego, US) according to the manufacturer's protocols. Samples which failed genotyping or with low call rate (, 95%, n = 11), with excessive heterozygosity (defined as sample heterozygosity exceeding 3 standard deviations from the mean sample heterogzygosity; n = 3), with gender discrepancies (n = 2) were excluded, as were cryptically related samples identified by the identity-by-state (IBS) (n = 41) and population structure in the principal components analyses (PCA) (n = 6). The criteria to define cryptically related samples and outliers with population structure in the discovery cohorts are described in the following paragraph. After the removal of the samples, SNP QC was then applied on a total of 579,999 autosomal SNPs for the 1,889 post-QC samples. SNPs were excluded based on (i) high rates of missingness (. 5%) (n = 26,437); (ii) monomorphism or minor allele frequency (MAF), 1% (n = 59,633); or (iii) genotype frequencies deviating from Hardy-Weinberg Equilibrium (HWE) defined as HWE P-value, 10^{2} 6 (n = 1,821). This yielded 492,108 autosomal SNPs. Those individuals with missing data on phenotypes were further removed (n = 29). Finally, 492,108 SNPs in 1,860 samples were available for analyses.

For SCORM, 1,116 DNA samples (1,037 from buccal swab and 79 from saliva) were genotyped on the Illumina HumanHap 550 Beadchips and 550 Duo Beadarrays. A total of 108 samples were excluded, comprising (i) 70 samples with call rates below 98%; (ii) 6 with poor genotyping quality; (iii) 11 samples identified from sibships; (iv) 18 with inconsistent gender information; and (v) 3 due to population structure. This left a total of 1,008 samples for further SNP QC. Based on 514,849 autosomal SNPs, we excluded 32,669 markers if they had missing genotype calls . 5%, MAF, 1%, or significantly deviated from HWE (P, 10^{2} 6) [14]. A final set of 929 samples with 482,180 post-QC SNPs and completed AL measurement were included in analyses.

For SiMES, 3,072 DNA samples were genotyped using the Illumina Human 610 Quad Beadchips. The detailed QC procedures were provided elsewhere [68]. In brief, we omitted a total of 530 individuals due to: (i) subpopulation structure (n = 170); (ii) cryptic relatedness (n = 279); (iii) excessive heterozygosity or high missingness rate . 5% (n = 37); and (iv) gender discrepancy (n = 44). After the removal of the samples, SNP QC was then applied on a total of 579,999 autosomal SNPs for the 2,542 post-QC samples. SNPs were excluded based on: (i) high rates of missingness (. 5%) (n = 26,343); (ii) monomorphism or MAF, 1% (n = 34,891); or (iii) genotype frequencies deviating from HWE (P, 10^{2} 6) (n = 3,645). This yielded 515,120 SNPs after the same SNP QC criteria. Individuals without valid measurements for AL were further removed (n = 387). After the above filtering criteria, 515,120 SNPs in 2,155 samples were available for association analyses.

In our discovery cohorts, IBS was estimated with the genome-wide SNP data using PLINK software to assess the degree of recent shared ancestry for a pair of individuals [69]. For a pair of putatively-related samples defined as an identity by descent (IBD) value greater than 0.185 [70], we removed one individual from each pair of monzygotic twins/ duplicates, parent-offspring or full-siblings etc. Population structure was ascertained using PCA with the EIGENSTRAT program and genetic outliers were defined as individuals whose ancestry was at least 6 standard deviations from the mean on one of the top ten inferred axes of variation [71].

For SiMES Malays, we also excluded the samples falling in the main clusters of PCA plots of the Chinese and Indians ethnic groups, as described in the previous study [68]. In SiMES, we noticed some degree of admixture in genetic ancestry of Malays and thus adjusted for ancestry along the top five axes of variation, as the spread of principal component scores was greater for the top five eigenvectors in the bivariate plots of PCA (Figure S3), The top ten principal components explained a small percentage of the global genetic variability of 1.3% while top five explained 1.0%, suggesting, all together, they had minimal effects on our association analyses.

Validation cohorts for high myopia

High myopia cases in the Japan dataset 1 were genotyped using Illumina Human-Hap550 and 660 chips [13], while controls in the Japan dataset 1 were genotyped on Illumina Human-Hap610 chips. Subjects in the Japan dataset 2 were genotyped on the Affymetrix GeneChip Human Mapping 500 K Array Set (Affymetrix Inc., Santa Clara, US). For SNPs not available on the Affymetric chips (rs43737678, rs10779363 and rs7544369), genotyping was performed with TaqMan 59exonuclease assays using primers supplied by Applied Biosystems (Foster City, US). The probe fluorescence signal was detected using the TaqMan Assay for Real-Time PCR (7500 Fast Real-Time PCR System, Applied Biosystems).

Gene expression in a mouse model of myopia

Experimental myopia was induced in B6 wild-type (WT) mice (n = 36) by applying a 2 15.00 D spectacle lens on the right eye (experimental eye) for 6 weeks since post-natal day 10. The left eyes were uncovered and served as contra-lateral fellow eyes. Age matched naive mice eyes were used as independent control eyes (n = 36). Each eye was refracted weekly using the automated infrared photorefractor as described previously [72]. AL was measured by AC- Master, Optic low coherence interferometry (Carl-Zeiss), in-vivo at 2, 4 and 6 weeks after the induction of myopia [73]. The minus-lens-induced eyes after six weeks were significantly associated with increased AL and myopic shift in refraction of , 2 5.00 D as compared to independent control eyes (n = 36, P = 3.006 10^{2} 6 for AL, and 2.056 10^{2} 4 for refraction). Eye tissues were collected at 6 weeks post myopia induction for further analyses.

Total RNA was isolated from pooled cryogenically ground mouse neural retina (retina), retinal pigment epithelium (RPE) and sclera for three batches using TRIzol Reagent (Invitrogen, Carlsbad, CA) with each batch (n = 6) comprising the myopic eye, fellow eye and control eye. RNA concentration and quality were assessed by the absorbance at 260 nm and the ratio of absorbance ratio at 260 and 280 nm respectively, using Nanodrop ND-1000 Spectrophotometer (Nanodrop Technologies, Wilmington, DE). RNA was purified using the RNeasy Mini kit (Qiagen, GmbH).

500 ng of purifed RNA was reverse-transcribed into cDNA using random primers and reagents from iScriptTM select cDNA synthesis kit (Bio-rad Laboratories, Hercules, CA). The pseudogene ZC3H11B (zinc finger CCCH type containing 11B) is not characterized in the mouse genome, therefore we examined a similar gene ZC3H11A (zinc finger CCCH type containing 11A) in mice. ZC3H11A in mice and ZC3H11B in humans are highly conserved with 79% nucleotide similarity by BLAST alignment analysis (http://blast.ncbi.nlm.nih.gov). We used quantitative Real-Time PCR (qRT-PCR) to validate the gene expression. qRT-PCR primers (Table S5) were designed using ProbeFinder 2.45 (Roche Applied Science, Indianapolis, IN) and this was performed using a Lightcycler 480 Probe Master (Roche Applied Science, Indianapolis, IN). The reaction was run in a Lightcycler 480 for 45 cycles under the following conditions: 95uC for 10 s, 56uC for 10 s and 72uC for 30 s. Gene expressions in the retina, RPE and sclera after six weeks of myopic eyes and the fellow eyes were compared to the control eyes. Glyceraldehyde 3-phosphate dehydrogenase (GAPDH) was used as an endogenous internal control.

Immunohistochemistry

Whole mouse eyes (6 weeks minus lens treated myopic, contralateral fellow and independent control eyes, n = 6 per type) were embedded in frozen tissue matrix compound at 2 20uC for 1 hour. Prepared tissue blocks were sectioned with a cryostat at 6 microns thicknesses and collected on clean polysine^{TM} glass slides. Slides with the sections were air dried at room temperature (RT) for 1 hour and fixed with 4% para-formaldehyde for 10 min. After washing 3X with 1x PBS for 5 minutes, 4% bovine serum albumin (BSA) diluted with 1x PBS was added as a blocking buffer. The slides were then covered and incubated for 1 hour at RT in a humid chamber. After rinsing with 1x PBS, a specific primary antibody raised in rabbit against ZC3H11A, SLC30A10 and raised in goat against LYPLAL1 (Abcam, Cambridge, UK) diluted (1:200) with 4% BSA was added and incubated further at 4uC in a humid chamber overnight. After washing 3X with 1x PBS for 10 min, fluorescein-labeled goat anti-rabbit secondary antibody (1:800, Invitrogen-Molecular Probes, Eugene, OR) and fluorescein-labeled rabbit anti-goat secondary antibody (1:800, Santa Cruz Biotechnology, Inc. CA, USA) was applied respectively and incubated for 90 min at RT. After washing and air-drying, slides were mounted with antifade medium containing DAPI (4,6-diamidino-2-phenylindole; Vectashield, Vector Laboratories, Burlingame, CA) to visualize the cell nuclei. Sections incubated with 4% BSA and omitted primary antibody were used as a negative control. A fluorescence microscope (Axioplan 2; Carl Zeiss Meditec GmbH, Oberkochen, Germany) was used to examine the slides and capture images. Experiments were repeated in duplicates from three different samples.

Gene expression in human tissues

GAPDH, ZC3H11B, SLC30A10, and LYLPLAL1 were run using 10 ul reactions with Qiagen's PCR products consisting of 1.26 ul H_2O, 1.0 ul 10X buffer, 1.0 ul dNTPs, 0.3 ul MgCl, 2.0 ul Q-Solution, 0.06 ul taq polymerase, 1.0 ul forward primer, 1.0 ul reverse primer and 1.5.0 ul cDNA. The reactions were run on a Eppendorf Mastercycler Pro S thermocycler with touchdown PCR ramping down 1uC per cycle from 72uC to 55uC followed by 50 cycles of 94uC for 0:30, 55uC for 0:30 and 72uC for 0:30 with a final elongation of 7:00 at 72uC. All primer sets were designed using Primer3 [74]. The gel electrophoresis was run on a 2% agarose gel at 70 volts for 35 minutes. The primers were run on a custom tissue panel including Clontech's Human MTC Panel I, Fetal MTC Panel I and an ocular tissue panel. The adult ocular samples were obtained from normal eyes of an 82-year-old Caucasian female from the North Carolina Eye Bank, Winston-Salem, North Carolina, USA. The fetal ocular samples were from 24-week fetal eyes obtained by Advanced Bioscience Resources Inc., Alameda, California, USA. All adult ocular samples were stored in Qiagen's RNAlater within 6.5 hours of collection and shipped on ice overnight to the lab. Fetal eyes were preserved in RNAlater within minutes of harvesting and shipped over night on ice. Whole globes were dissected on the arrival day. Isolated tissues were snap-frozen and stored at 2 80uC until RNA extraction. RNA was extracted from each tissue sample independently using the Ambion mirVana total RNA extraction kit. The tissue samples were homogenized in Ambion lysis buffer using an Omni Bead Ruptor Tissue Homogenizer per protocol. Reverse transcription reactions were performed with Invitrogen SuperScript III First-Strand Synthesis kit.

Statistical analysis

The primary analysis was performed on the AL quantitative trait. As a strong correlation exists in AL measurements from both eyes (r. 0.9), we used the mean AL across both eyes in the GWAS analysis, as was recommended in a review [75]. Linear regression was used to interrogate the association of each SNP with AL after adjusting for age, gender, height and level of education, under the assumption of an additive genetic effect where the genotypes of each SNP are coded numerically as 0, 1 and 2 for the number of minor alleles carried. In addition, for SiMES, the top five principal components of genetic ancestry from the EIGENSTRAT PCA were also included as covariates to account for the effects of population substructure as described in genotype QC section [60]. Association tests between each genetic marker and phenotype were carried out using PLINK software [69] (version 1.07). Analyses were also repeated without adjustment for education level or height for the purpose of comparison.

In the discovery phase, we conducted a meta-analysis of GWAS results from 3 cohorts for AL using a weighted-inverse variance approach by fixed-effect modeling in METAL (http://www.sph.umich.edu/csg/abecasis/metal). In the secondary analyses, SNPs that have been identified from the primary analyses were tested for association with high myopia onset (as a binary trait) and SE (as a quantitative trait). For Singapore cohorts, the association analyses adjusted for the same covariates as the primary analyses within a linear regression and logistic regression framework respectively. For Japan case-control datasets, only age and gender were included as covariates in the model for high myopia, as the other covariates were not available.

The regional association plots were constructed by SNAP (http://www.broadinstitute.org/mpg/snap). Haploview 4.1 (http://www.broad.mit.edu/mpg/haploview) was used to visualize the LD of the genomic regions. Genotyping quality of all reported SNPs has been visually evaluated by the intensity clusterplots. The coordinates reported in this paper are on NCB136 (hg18).

For functional studies in the myopic mouse model, gene expression of all three identified genes in control and experimental groups was quantified using the $2^{2\,DDCt}$ method [76]. The standard student's t-test was performed to determine the significance of the relative fold change of mRNA between the myopic eyes of the experimental mice with the independent age-matched controls.

Supporting Information

Figure S1 Principal Component Analysis (PCA) of discovery cohorts SCES, SCORM and SiMES with respect to the four population panels in phase 2 of the HapMap samples (CEU - European, YRI ☒African, CHB ☒Chinese, JPT ☒Japanese) (A), and with respect to two reference population panels CHB and JPT (B☒D). (A) Principal components 1 versus 2; the principal components (PCs) were calculated with SCES, SCORM, SiMES and four HapMap panels on the thinned set of 102,122 SNPs (r^2, 0.2). (B) Principal components 1 versus 2; (C) Principal components 1 versus 3; (D) Principal components 1 versus 4. For (B☒D), the PCs were calculated with SCES, SCORM, SiMES and HapMap Asian population panels on the thinned set of 86,516 SNPs (r^2, 0.2).
(PDF)

Figure S2 Quantile-Quantile (Q-Q) plots of P-values for association between all SNPs and AL in the individual cohort (A) SCES, (B) SCORM, (C) SiMES, and combined meta-analysis of the discovery cohorts (D) SCES+SCORM+SiMES.
(PDF)

Figure S3 Principal Component Analysis (PCA) was performed in SiMES to assess the extent of population structure. Each figure represents a bivariate plot of two principal components from the

PCA of genetic diversity within SiMES on the thinned set of 83,585 SNPs (r^2, 0.2). The first 5 principal components were used as covariates to account for population structure.
(PDF)

Table S1 Characteristics of high myopia cases and controls in three Singapore cohorts.
(DOCX)

Table S2 Association between genetic variants at chromosome 1q41 and high myopia in the meta-analysis of five cohorts.
(DOCX)

Table S3 Association between genetic variants at chromosome 1q41 and spherical equivalent (SE) in the meta-analysis of three Asian cohorts.
(DOCX)

Table S4 Definitions and numbers of high-myopia cases and controls used in the main and supplementary association analyses for high myopia.
(DOCX)

Table S5 Gene accession number in the nucleotide sequence database (NCBI), and qRT-PCR primer sequences in mice genome.
(DOCX)

Acknowledgments

We wish to express our gratitude to all the normal subjects and patients who volunteered to take part in this study. We acknowledge the Genome Institute of Singapore for genotyping all the samples collected from the cohort studies in Singapore and the research team of the Singapore Eye Research Institute who phenotyped the subjects.

Author Contributions

Conceived and designed the experiments: TLY T-YW Y-YT S-MS. Performed the experiments: VAB AM IN WL CEHH FH YZ DC HI KY. Analyzed the data: QF VAB XZ C-YC. Contributed reagents/materials/analysis tools: C-CK L-KG Y-JL KO-M KM FM EV MS NM RWB E-ST NY TA TLY T-YW Y-YT S-MS. Wrote the paper: QF VAB Y-YT S-MS. Critically reviewed the manuscript: C-YC C-CK L-KG E-ST TLY T-YW.

References

1. Pan CW, Ramamurthy D, Saw SM (2012) Worldwide prevalence and risk factors for myopia. Ophthalmic Physiol Opt 32: 3–6.
2. Saw SM, Chua WH, Gazzard G, Koh D, Tan DT, et al. (2005) Eye growth changes in myopic children in Singapore. Br J Ophthalmol 89: 1489–1494.
3. Wong TY, Foster PJ, Hee J, Ng TP, Tielsch JM, et al. (2000) Prevalence and risk factors for refractive errors in adult Chinese in Singapore. Invest Ophthalmol Vis Sci 41: 2486–2494.
4. Saw SM, Gazzard G, Shih-Yen EC, Chua WH (2005) Myopia and associated pathological complications. Ophthalmic Physiol Opt 25: 381–391.
5. McBrien NA, Gentle A (2003) Role of the sclera in the development and pathological complications of myopia. Prog Retin Eye Res 22: 307–338.
6. Saw SM, Katz J, Schein OD, Chew SJ, Chan TK (1996) Epidemiology of myopia. Epidemiol Rev 18: 175–187.
7. Hammond CJ, Snieder H, Gilbert CE, Spector TD (2001) Genes and environment in refractive error: the twin eye study. Invest Ophthalmol Vis Sci 42: 1232–1236.
8. Klein AP, Suktitipat B, Duggal P, Lee KE, Klein R, et al. (2009) Heritability analysis of spherical equivalent, axial length, corneal curvature, and anterior chamber depth in the Beaver Dam Eye Study. Arch Ophthalmol 127: 649–655.
9. Lyhne N, Sjolie AK, Kyvik KO, Green A (2001) The importance of genes and environment for ocular refraction and its determiners: a population based study among 20–45 year old twins. Br J Ophthalmol 85: 1470–1476.
10. Sanfilippo PG, Hewitt AW, Hammond CJ, Mackey DA (2010) The heritability of ocular traits. Surv Ophthalmol 55: 561–583.
11. Solouki AM, Verhoeven VJ, van Duijn CM, Verkerk AJ, Ikram MK, et al. (2010) A genome-wide association study identifies a susceptibility locus for refractive errors and myopia at 15q14. Nat Genet 42: 897–901.
12. Hysi PG, Young TL, Mackey DA, Andrew T, Fernandez-Medarde A, et al. (2010) A genome-wide association study for myopia and refractive error identifies a susceptibility locus at 15q25. Nat Genet 42: 902–905.
13. Nakanishi H, Yamada R, Gotoh N, Hayashi H, Yamashiro K, et al. (2009) A genome-wide association analysis identified a novel susceptible locus for pathological myopia at 11q24.1. PLoS Genet 5: e1000660. doi:10.1371/journal.pgen.1000660.
14. Li YJ, Goh L, Khor CC, Fan Q, Yu M, et al. (2011) Genome-wide association studies reveal genetic variants in CTNND2 for high myopia in Singapore Chinese. Ophthalmology 118: 368–375.
15. Li Z, Qu J, Xu X, Zhou X, Zou H, et al. (2011) A genome-wide association study reveals association between common variants in an intergenic region of 4q25 and high-grade myopia in the Chinese Han population. Hum Mol Genet 20: 2861–2868.
16. Shi Y, Qu J, Zhang D, Zhao P, Zhang Q, et al. (2011) Genetic variants at 13q12.12 are associated with high myopia in the han chinese population. Am J Hum Genet 88: 805–813.
17. Saw SM, Shankar A, Tan SB, Taylor H, Tan DT, et al. (2006) A cohort study of incident myopia in Singaporean children. Invest Ophthalmol Vis Sci 47: 1839–1844.
18. Dirani M, Shekar SN, Baird PN (2008) Evidence of shared genes in refraction and axial length: the Genes in Myopia (GEM) twin study. Invest Ophthalmol Vis Sci 49: 4336–4339.
19. Biino G, Palmas MA, Corona C, Prodi D, Fanciulli M, et al. (2005) Ocular refraction: heritability and genome-wide search for eye morphometry traits in an isolated Sardinian population. Hum Genet 116: 152–159.
20. Zhu G, Hewitt AW, Ruddle JB, Kearns LS, Brown SA, et al. (2008) Genetic dissection of myopia: evidence for linkage of ocular axial length to chromosome 5q. Ophthalmology 115: 1053–1057 e1052.
21. Leung KW, Liu M, Xu X, Seiler MJ, Barnstable CJ, et al. (2008) Expression of ZnT and ZIP zinc transporters in the human RPE and their regulation by neurotrophic factors. Invest Ophthalmol Vis Sci 49: 1221–1231.
22. Liang J, Song W, Tromp G, Kolattukudy PE, Fu M (2008) Genome-wide survey and expression profiling of CCCH-zinc finger family reveals a functional module in macrophage activation. PLoS ONE 3: e2880. doi:10.1371/journal.pone.0002880.
23. Poliseno L, Salmena L, Zhang J, Carver B, Haveman WJ, et al. (2010) A coding-independent function of gene and pseudogene mRNAs regulates tumour biology. Nature 465: 1033–1038.
24. Salmena L, Poliseno L, Tay Y, Kats L, Pandolfi PP (2011) A ceRNA Hypothesis: The Rosetta Stone of a Hidden RNA Language? Cell 146: 353–358.
25. D'Errico I, Gadaleta G, Saccone C (2004) Pseudogenes in metazoa: origin and features. Brief Funct Genomic Proteomic 3: 157–167.
26. Shi Y, Li Y, Zhang D, Zhang H, Lu F, et al. (2011) Exome sequencing identifies ZNF644 mutations in high myopia. PLoS Genet 7: e1002084. doi:10.1371/journal.pgen.1002084.
27. Schippert R, Burkhardt E, Feldkaemper M, Schaeffel F (2007) Relative axial myopia in Egr-1 (ZENK) knockout mice. Invest Ophthalmol Vis Sci 48: 11–17.
28. Laity JH, Lee BM, Wright PE (2001) Zinc finger proteins: new insights into structural and functional diversity. Curr Opin Struct Biol 11: 39–46.
29. Fischer AJ, McGuire JJ, Schaeffel F, Stell WK (1999) Light- and focus-dependent expression of the transcription factor ZENK in the chick retina. Nat Neurosci 2: 706–712.
30. Bitzer M, Schaeffel F (2002) Defocus-induced changes in ZENK expression in the chicken retina. Invest Ophthalmol Vis Sci 43: 246–252.
31. Simon P, Feldkaemper M, Bitzer M, Ohngemach S, Schaeffel F (2004) Early transcriptional changes of retinal and choroidal TGFbeta-2, RALDH-2, and ZENK following imposed positive and negative defocus in chickens. Mol Vis 10: 588–597.
32. Liu C, Adamson E, Mercola D (1996) Transcription factor EGR-1 suppresses the growth and transformation of human HT-1080 fibrosarcoma cells by induction of transforming growth factor beta 1. Proc Natl Acad Sci U S A 93: 11831–11836.
33. Baron V, Adamson ED, Calogero A, Ragona G, Mercola D (2006) The transcription factor Egr1 is a direct regulator of multiple tumor suppressors including TGFbeta1, PTEN, p53, and fibronectin. Cancer Gene Ther 13: 115–124.
34. Khor CC, Fan Q, Goh L, Tan D, Young TL, et al. (2010) Support for TGFB1 as a susceptibility gene for high myopia in individuals of Chinese descent. Arch Ophthalmol 128: 1081–1084.
35. Zha Y, Leung KH, Lo KK, Fung WY, Ng PW, et al. (2009) TGFB1 as a susceptibility gene for high myopia: a replication study with new findings. Arch Ophthalmol 127: 541–548.
36. Seve M, Chimienti F, Devergnas S, Favier A (2004) In silico identification and expression of SLC30 family genes: an expressed sequence tag data mining strategy for the characterization of zinc transporters' tissue expression. BMC Genomics 5: 32.
37. van Leeuwen R, Boekhoorn S, Vingerling JR, Witteman JC, Klaver CC, et al. (2005) Dietary intake of antioxidants and risk of age-related macular degeneration. JAMA 294: 3101–3107.
38. Ugarte M, Osborne NN (2001) Zinc in the retina. Prog Neurobiol 64: 219–249.

39. Huibi X, Kaixun H, Qiuhua G, Yushan Z, Xiuxian H (2001) Prevention of axial elongation in myopia by the trace element zinc. Biol Trace Elem Res 79: 39–47.
40. Steinberg GR, Kemp BE, Watt MJ (2007) Adipocyte triglyceride lipase expression in human obesity. Am J Physiol Endocrinol Metab 293: E958–964.
41. Heid IM, Jackson AU, Randall JC, Winkler TW, Qi L, et al. (2010) Meta-analysis identifies 13 new loci associated with waist-hip ratio and reveals sexual dimorphism in the genetic basis of fat distribution. Nat Genet 42: 949–960.
42. Lindgren CM, Heid IM, Randall JC, Lamina C, Steinthorsdottir V, et al. (2009) Genome-wide association scan meta-analysis identifies three Loci influencing adiposity and fat distribution. PLoS Genet 5: e1000508. doi:10.1371/journal.pgen.1000508.
43. Cordain L, Eaton SB, Brand Miller J, Lindeberg S, Jensen C (2002) An evolutionary analysis of the aetiology and pathogenesis of juvenile-onset myopia. Acta Ophthalmol Scand 80: 125–35.
44. Cordain L, Eades MR, Eades MD (2003) Hyperinsulinemic diseases of civilization: more than just Syndrome X. Comp Biochem Physiol A Mol Integr Physiol 136: 95–112.
45. Lim LS, Gazzard G, Low YL, Choo R, Tan DT, et al. (2010) Dietary factors, myopia, and axial dimensions in children. Ophthalmology 117: 993–997 e994.
46. Gao H, Frost MR, Siegwart JT, Jr., Norton TT (2011) Patterns of mRNA and protein expression during *minus-lens compensation* and recovery in tree shrew sclera. Mol Vis 17: 903–919.
47. Klein AP, Duggal P, Lee KE, Klein R, Bailey-Wilson JE, et al. (2007) Confirmation of linkage to ocular refraction on chromosome 22q and identification of a novel linkage region on 1q. Arch Ophthalmol 125: 80–85.
48. Klein AP, Duggal P, Lee KE, Cheng CY, Klein R, et al. (2011) Linkage analysis of quantitative refraction and refractive errors in the beaver dam eye study. Invest Ophthalmol Vis Sci 52: 5220–5225.
49. Wong TY, Foster PJ, Johnson GJ, Seah SK (2003) Refractive errors, axial ocular dimensions, and age-related cataracts: the Tanjong Pagar survey. Invest Ophthalmol Vis Sci 44: 1479–1485.
50. Wu R, Wang JJ, Mitchell P, Lamoureux EL, Zheng Y, et al. (2010) Smoking, socioeconomic factors, and age-related cataract: The Singapore Malay Eye study. Arch Ophthalmol 128: 1029–1035.
51. Tokoro T (1988) On the definition of pathologic myopia in group studies. Acta Ophthalmol Suppl 185: 107–108.
52. Plomin R, Haworth CM, Davis OS (2009) Common disorders are quantitative traits. Nat Rev Genet 10: 872–878.
53. Hayashi H, Yamashiro K, Nakanishi H, Nakata I, Kurashige Y, et al. (2011) Association of 15q14 and 15q25 with High Myopia in Japanese. Invest Ophthalmol Vis Sci.
54. Dirani M, Shekar SN, Baird PN (2008) Adult-onset myopia: the Genes in Myopia (GEM) twin study. Invest Ophthalmol Vis Sci 49: 3324–3327.
55. Jensen H (1995) Myopia in teenagers. An eight-year follow-up study on myopia progression and risk factors. Acta Ophthalmol Scand 73: 389–93.
56. McCarthy MI, Hirschhorn JN (2008) Genome-wide association studies: potential next steps on a genetic journey. Hum Mol Genet 17: R156–165.
57. Teo YY, Small KS, Fry AE, Wu Y, Kwiatkowski DP, et al. (2009) Power consequences of linkage disequilibrium variation between populations. Genet Epidemiol 33: 128–35.
58. Ip JM, Huynh SC, Kifley A, Rose KA, Morgan IG, et al. (2007) Variation of the contribution from axial length and other oculometric parameters to refraction by age and ethnicity. Invest Ophthalmol Vis Sci 48: 4846–4853.
59. Lavanya R, Jeganathan VS, Zheng Y, Raju P, Cheung N, et al. (2009) Methodology of the Singapore Indian Chinese Cohort (SICC) eye study: quantifying ethnic variations in the epidemiology of eye diseases in Asians. Ophthalmic Epidemiol 16: 325–36.
60. Fan Q, Zhou X, Khor CC, Cheng CY, Goh LK, et al. (2011) Genome-wide meta-analysis of five Asian cohorts identifies PDGFRA as a susceptibility locus for corneal astigmatism. PLoS Genet 7: e1002402. doi:10.1371/journal.pgen.1002402.
61. Foong AW, Saw SM, Loo JL, Shen S, Loon SC, et al. (2007) Rationale and methodology for a population-based study of eye diseases in Malay people: The Singapore Malay eye study (SiMES). Ophthalmic Epidemiol 14: 25–35.
62. Vithana EN, Aung T, Khor CC, Cornes BK, Tay WT, et al. (2011) Collagen-related genes influence the glaucoma risk factor, central corneal thickness. Hum Mol Genet 20: 649–58.
63. Khor CC, Ramdas WD, Vithana EN, Cornes BK, Sim X, et al. (2011) Genome-wide association studies in Asians confirm the involvement of ATOH7 and TGFBR3, and further identify CARD10 as a novel locus influencing optic disc area. Hum Mol Genet 20: 1864–1872.
64. Grosvenor TP (2007) Primary care optometry. St. Louis, Mo: Butterworth-Heinemann/Elsevier. xiii, 510 p.
65. Schork NJ, Nath SK, Fallin D, Chakravarti A (2000) Linkage disequilibrium analysis of biallelic DNA markers, human quantitative trait loci, and threshold-defined case and control subjects. Am J Hum Genet 67: 1208–1218.
66. Saw SM, Chan YH, Wong WL, Shankar A, Sandar M, et al. (2008) Prevalence and risk factors for refractive errors in the Singapore Malay Eye Survey. Ophthalmology 115: 1713–1719.
67. Fan DS, Lam DS, Lam RF, Lau JT, Chong KS, et al. (2004) Prevalence, incidence, and progression of myopia of school children in Hong Kong. Invest Ophthalmol Vis Sci 45: 1071–1075.
68. Sim X, Ong RT, Suo C, Tay WT, Liu J, et al. (2011) Transferability of type 2 diabetes implicated loci in multi-ethnic cohorts from Southeast Asia. PLoS Genet 7: e1001363. doi:10.1371/journal.pgen.1001363.
69. Purcell S, Neale B, Todd-Brown K, Thomas L, Ferreira MA, et al. (2007) PLINK: a tool set for whole-genome association and population-based linkage analyses. Am J Hum Genet 81: 559–575.
70. Anderson CA, Pettersson FH, Clarke GM, Cardon LR, Morris AP, et al. (2010) Data quality control in genetic case-control association studies. Nat Protoc 5: 1564–1573.
71. Price AL, Patterson NJ, Plenge RM, Weinblatt ME, Shadick NA, et al. (2006) Principal components analysis corrects for stratification in genome-wide association studies. Nat Genet 38: 904–909.
72. Schaeffel F, Burkhardt E, Howland HC, Williams RW (2004) Measurement of refractive state and deprivation myopia in two strains of mice. Optom Vis Sci 81: 99–110.
73. Barathi VA, Boopathi VG, Yap EP, Beuerman RW (2008) Two models of experimental myopia in the mouse. Vision Res 48: 904–916.
74. Rozen S, Skaletsky H (2000) Primer3 on the WWW for general users and for biologist programmers. Methods Mol Biol 132: 365–386.
75. Fan Q, Teo YY, Saw SM (2011) Application of advanced statistics in ophthalmology. Invest Ophthalmol Vis Sci 52: 6059–6065.
76. Brink N, Szamel M, Young AR, Wittern KP, Bergemann J (2000) Comparative quantification of IL-1beta, IL-10, IL-10r, TNFalpha and IL-7 mRNA levels in UV-irradiated human skin in vivo. Inflamm Res 49: 290–296.

Case Reports in Ophthalmology

Case Rep Ophthalmol 2014;5:34–37

DOI: 10.1159/000358426
Published online: January 22, 2014

1663–2699/14/0051–0034$39.50/0
www.karger.com/cop

Karger Open access

A Case of Choroidal Neovascularization Secondary to Unilateral Retinal Pigment Epithelium Dysgenesis

Tsuyoshi Shimoyama[a, b] Hisanori Imai[a, b] Shigeru Honda[a] Akira Negi[a]

[a]Division of Ophthalmology, Department of Organ Therapeutics, Kobe University Graduate School of Medicine, and [b]Department of Ophthalmology, Kobe Kaisei Hospital, Kobe, Japan

Key Words

Unilateral retinal pigment epithelium dysgenesis · Anti-VEGF · Bevacizumab · Choroidal neovascularization · Triamcinolone · Fundus autofluorescence

Abstract

Aim: To report a case of choroidal neovascularization secondary to unilateral retinal pigment epithelium dysgenesis (URPED), which was resistant to posterior subtenon injection of triamcinolone acetonide (STTA) and intravitreal bevacizumab injection (IVB). ***Case Report:*** An 8-year-old boy was referred to us because of a unilateral unique clinical appearance on funduscopic examination in his left eye (OS). A geometric lesion at the retinal pigment epithelium level of the interpapillomacular area was disclosed OS. The optic nerve was slightly hyperemic OS. Findings from the right fundus examination were normal. Based on these characteristic findings, he was diagnosed as having URPED. Best corrected Landolt ring chart visual acuity (BCVA) was 1.0 in both eyes. Twenty-three months after the first visit, the patient presented with visual disturbance OS. Funduscopic examination showed an expansion of the geometric lesion and the development of a subfoveal choroidal neovascularization (CNV). BCVA was 0.4 OS. Two-time STTA (40 mg/1 ml) was performed at the onset of CNV and 6 months later, and additional IVB (1.25 mg/0.05 ml) was done 10 months later for the treatment of CNV, but the geometric lesion and CNV were resistant to the treatment and continued to expand. Seven years after the first visit, the geometric lesion and the CNV kept expanding steadily. ***Conclusion:*** URPED is a rare clinical entity, and the prognosis of this disease is still unclear. The visual prognosis may depend on whether CNV fully develops.

Hisanori Imai, MD, PhD
Department of Ophthalmology
Kobe Kaisei Hospital
3-11-15 Shinoharakitamati, Nada-ku, Kobe 657-0068 (Japan)
E-Mail imai@kobe-kaisei.org

Case Reports in Ophthalmology

Case Rep Ophthalmol 2014;5:34–37
DOI: 10.1159/000358426

Introduction

Unilateral retinal pigment epithelium dysgenesis (URPED) is a rare clinical entity [1–3]. It is characterized by a unilateral occurrence in young patients and consists of a round affected area with a distinct scalloped margin of reticular retinal pigment epithelium (RPE) hyperplasia, mid-lesion lacunae of RPE hyperplasia, central thinning and atrophy of RPE. The findings of fundus autofluorescence (FAF) and fluorescein angiography (FA) are the most important when diagnosing URPED. The visual prognosis of URPED is still unclear, but it may depend on whether choroidal neovascularization (CNV) will develop [1].

In this report, we present a case of CNV associated with URPED, which was resistant to the treatment with posterior subtenon injection of triamcinolone acetonide (STTA) and intravitreal bevacizumab injection (IVB).

Case Report

An 8-year-old boy was referred to us because of a unilateral unique funduscopic appearance in the left eye (OS). Funduscopic findings revealed a geometric lesion at the RPE level of the interpapillomacular area, contiguous with the slightly hyperemic optic nerve (fig. 1). The lesion was composed of marginal RPE hyperplasia and atrophic RPE in its center. Findings from the right fundus examination were normal. Based on these characteristic findings, the patient was diagnosed with URPED. Best corrected Landolt ring chart visual acuity (BCVA) was 1.0 in both eyes. Twenty-three months after the first visit, he presented with visual disturbance OS. Funduscopic examination showed enlargement of the lesion and development of subfoveal CNV (fig. 2). FA findings revealed hypofluorescence from RPE hyperplasia, hyperfluorescence from RPE atrophy and dye leakage from the optic nerve and CNV (fig. 2). Optical coherence tomography (OCT) revealed type 2 CNV, but the exudative change was not obvious (fig. 2). The patient's BCVA was 0.4 OS. Two-time STTA (40 mg/1 ml) was performed at the onset of CNV and 6 months later. Additional IVB (1.25 mg/0.05 ml) was performed 10 months later for the treatment of CNV. Both STTA and IVB were performed with the written informed consent from both the patient and his father as well as with an approval of the institutional review board of Kobe University of Medicine and the Tenets of the Declaration of Helsinki. Despite the treatment, the geometric lesion and CNV were resistant to the treatment and expanded gradually. Seven years after the first visit, the geometric lesion and the CNV kept expanding steadily, and new CNV developed at the inferior retina (fig. 3).

Discussion

Cohen et al. [2] first reported 4 cases of this unique fundus lesion in 2002. In their study, 2 of 4 cases were complicated by CNV. Finally, in 2009, they proposed naming this disorder 'URPED' and reported that 2 of 9 cases were affected by CNV [1]. We believe that this is the first follow-up report which can provide new clinical information about this disease because Cohen et al. [1, 2] did not mention the course of CNV treatment.

In our case, CNV did not respond to both STTA and IVB. Systemic steroids, immunosuppressants or additional STTA and IVB might be effective to achieve the quieting effect of this highly active CNV, but we did not impose them because the patient was still experiencing periods of growth. Generally, regardless of the treatment, CNV suppresses eventually with

RPE proliferation, which is one of the remodeling processes of wound repairing. In our case, we could not observe RPE proliferation around CNV during the follow-up period. On the contrary, new CNV developed at the inferior retina. Furthermore, the geometric lesion was significantly enlarged over the RPE hyperplasia. These findings may suggest that the congenital RPE malfunction, which spreads across a wide area of the fundus, is the underlying reason for the development of this disease.

Our case is unique because we observed the hyperemic optic nerve OS at the first visit. In the previous report, Cohen et al. [1] stated that the affected area is usually contiguous with the optic nerve, but they did not mention the condition of the optic nerve itself. It is possible that the inflammation of the optic nerve is one of the triggers in the development of this unique pattern of the fundus.

To summarize, we propose that patients who develop CNV secondary to URPED should be informed carefully and always be followed up for treatment-resistant CNV.

References

1 Cohen SY, Fung AE, Tadayoni R, Massin P, Barbazetto I, Berthout A, Gayet P, Meunier I, Yannuzzi LA: Unilateral retinal pigment epithelium dysgenesis. Am J Ophthalmol 2009;148:914–919.
2 Cohen SY, Massin P, Quentel G: Clinicopathologic reports, case reports, and small case series: unilateral, idiopathic leopard-spot lesion of the retinal pigment epithelium. Arch Ophthalmol 2002;120:512–516.
3 Berthout A, Malthieu D, Taboureau E, Milazzo S: Unilateral idiopathic leopard-spot lesion of the retinal pigment epithelium: a fibroglial tractional complication (in French). J Fr Ophtalmol 2008;31:716.

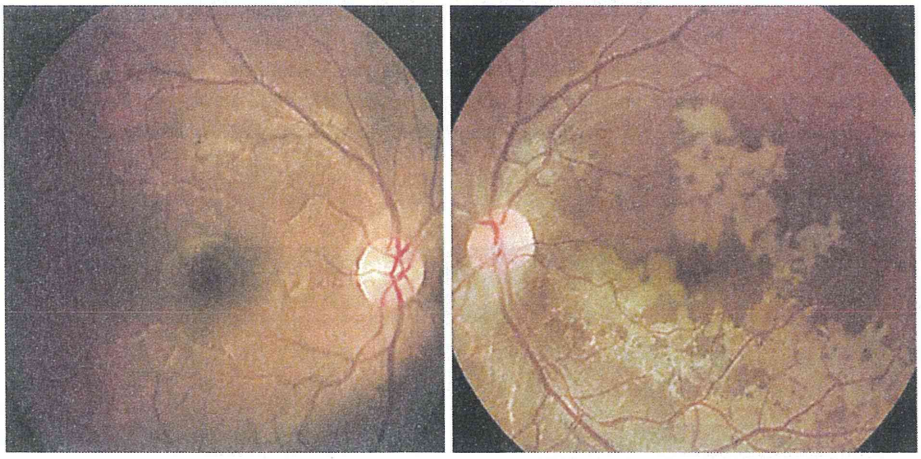

Fig. 1. Funduscopic findings at the first visit. Funduscopic findings OS revealed a geometric lesion at the RPE level of the interpapillomacular area, contiguous with the slightly hyperemic optic nerve. The lesion was composed of marginal RPE hyperplasia and atrophic RPE in its center. Findings from the right fundus examination were normal.

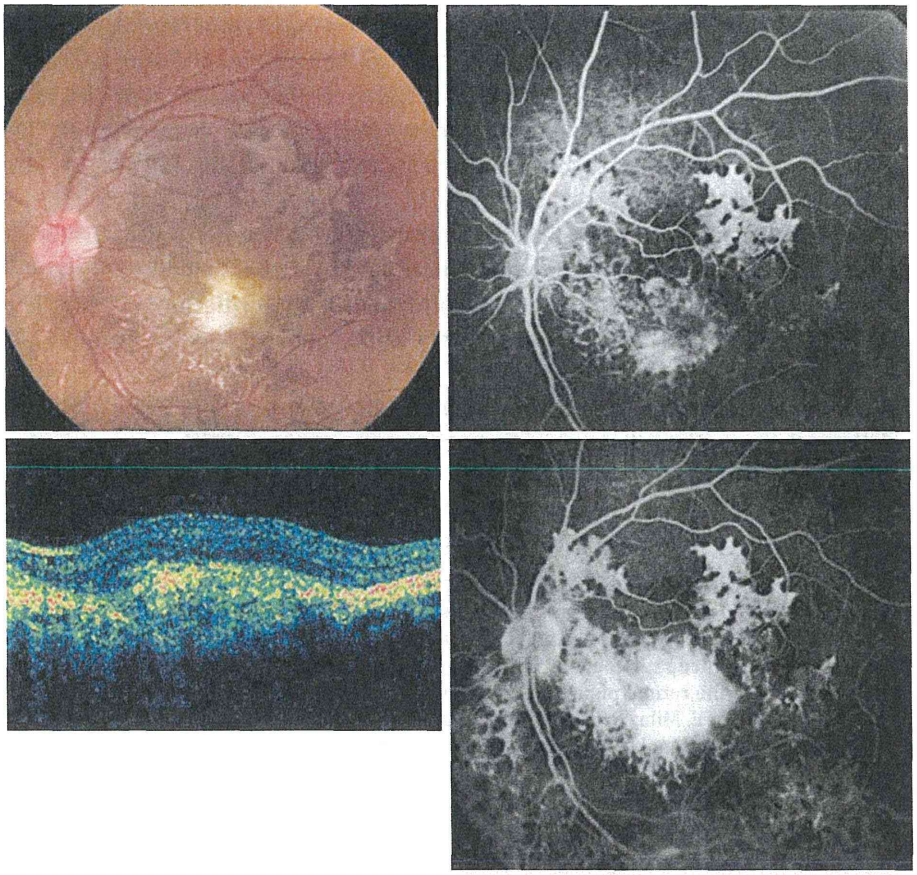

Fig. 2. Twenty-three months after the first visit, the enlargement of the lesion and the development of subfoveal CNV were observed (upper left: funduscopic findings, lower left: OCT findings). FA findings revealed dye leakage from the optic nerve and CNV (upper right: early-phase image, upper left: late-phase image).

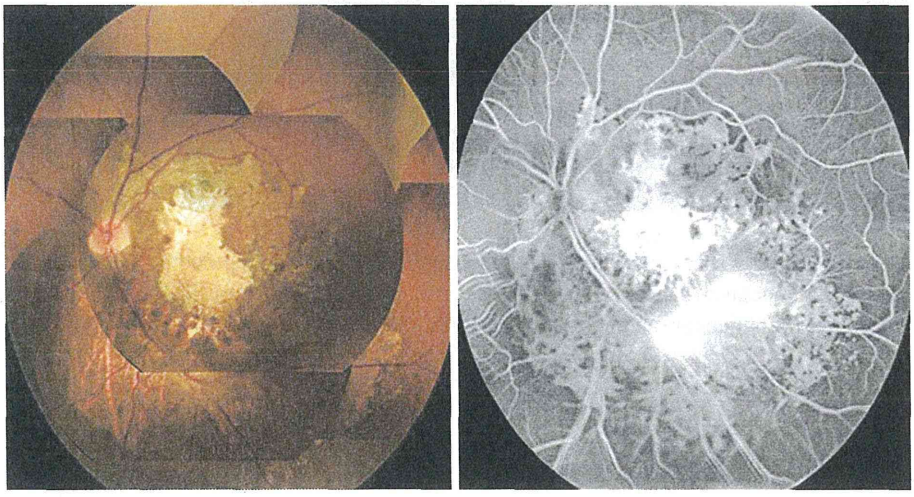

Fig. 3. Seven years after the first visit, the geometric lesion and CNV kept expanding steadily and new CNV developed at the inferior retina (upper: panoramic funduscopic findings, bottom: panoramic FA findings).

age values, so differences in OCT findings seems not to be attributable to aging and, (2) higher mean MMSE values seem to indicate that they are taking place in early stages of AD.

Based on our data, we propose that the first affected area of the retina in mild AD may be the macular area. As the neurodegeneration progresses, a significant decline in peripapillary RNFL thickness becomes apparent. However, whether or not the macula is really the first area involved in early AD, or simply the first place with enough RGCs to discern an effect deserves further investigation.

We suggest that with OCT we can detect consistent macular changes that can be of significant value for evaluating AD patients. The retina, being part of the central nervous system and offering easy accessibility, encourages its use as a potential biomarker for AD diagnosis and progression.

Elena S. Garcia-Martin, MSc[1]
Blanca Rojas, MD, PhD[1,2]
Ana I. Ramirez, PhD[1,3]
Rosa de Hoz, MD, PhD[1,3]
Juan J. Salazar, PhD[1,3]
Raquel Yubero, PhD[4]
Pedro Gil, MD, PhD[2,4]
Alberto Triviño, MD, PhD[1,2]
Jose M. Ramirez, MD, PhD[1,2]

[1]*Instituto de Investigaciones Oftalmológicas Ramón Castroviejo, Universidad Complutense de Madrid, Madrid, Spain;* [2]*Facultad de Medicina, Universidad Complutense de Madrid, Madrid, Spain;* [3]*Facultad de Óptica y Optometría, Universidad Complutense de Madrid, Madrid, Spain;* [4]*Hospital Clínico San Carlos, Madrid, Spain*

Financial Support: Redes temáticas de investigación cooperativa en salud (RETICs) Prevención, detección precoz y tratamiento de la patología ocular prevalente degenerativa y crónica (grant ISCIII RD12/0034/0002, Spanish Ministry of Science and Innovation). The author(s) have no proprietary or commercial interest in any materials discussed in this article.

References

1. Hinton DR, Sadun AA, Blanks JC, et al. Optic-nerve degeneration in Alzheimer's disease. N Engl J Med 1986;315:485–7.
2. He XF, Liu YT, Peng C, et al. Optical coherence tomography assessed retinal nerve fiber layer thickness in patients with Alzheimer's disease: a meta-analysis. Int J Ophthalmol 2012;5:401–5.
3. Blanks JC, Torigoe Y, Hinton DR, et al. Retinal pathology in Alzheimer's disease. I. ganglion cell loss in foveal/parafoveal retina. Neurobiol Aging 1996;17:377–84.
4. Tzekov RT, Mullan M. Vision function abnormalities in alzheimer's disease. Surv Ophthalmol 2013; In press: http://dx.doi.org/10.1016/j.survophthal.2013.10.002.
5. Koronyo Y, Salumbides BC, Black KL, et al. Alzheimer's disease in the retina: Imaging retinal aβ plaques for early diagnosis and therapy assessment. Neurodeg Dis 2012;10:285–93.

LAPTOP Study: A 24-Month Trial of Verteporfin Versus Ranibizumab for Polypoidal Choroidal Vasculopathy

Age-related macular degeneration (AMD) is a leading cause of vision loss in developed countries. Polypoidal choroidal vasculopathy (PCV) is a subtype of AMD characterized by polypoidal lesions and a branching vascular network visualized with indocyanine green angiography. Although the first-line treatment for AMD is well-established, the optimal treatment for PCV can differ from that of AMD and remains under debate.[1]

The administration of anti-vascular endothelial growth factor (VEGF) agents such as ranibizumab or aflibercept is the mainstay of the treatment of AMD. Meanwhile, the use of photodynamic therapy (PDT) alone or in combination with anti-VEGF agents is sometimes favored for patients with PCV because PDT efficiently induces regression of polyps that should be beneficial for long-term outcome.[2] Although the previous randomized study (EVEREST study) compared the use of ranibizumab and PDT for the treatment of PCV and concluded that PDT is more effective than ranibizumab in achieving regression of polyps,[3] the visual outcome was better in the ranibizumab monotherapy arm than in the PDT arm despite the lack of statistical power. Thus, no clear evidence exists for the treatment that yields the best visual outcome.

To address the issue, we conducted a 24-month trial: Ranibizumab (Lucentis) And Photodynamic Therapy On Polypoidal choroidal vasculopathy (LAPTOP) study and compared the vision-enhancing effect of ranibizumab and PDT in PCV. At 12 months, ranibizumab yielded a better visual outcome than did PDT.[4] We have now completed the 24-month study and report the results herein.

The methods used for the LAPTOP study have been reported previously.[4] Institutional review board/ethics committee approval was obtained at each institution. The study design adhered to the tenets of the Declaration of Helsinki and guidelines of Japanese Ministry of Health, Labor, and Welfare. Patients provided written, informed consent for participating in the study. The trial was registered with the Japan Medical Association Center for Clinical Trials on 2009-06-22 (ID: JMA-IIA00028). We randomized 97 patients with treatment-naïve PCV to either PDT or ranibizumab. In the PDT arm, we performed standard verteporfin PDT at baseline and applied retreatment when persistent fluorescein leakage was noted. In the ranibizumab arm, we performed 3 monthly intravitreal injections of ranibizumab 0.5 mg and additional treatments were given based on retreatment criteria as suggested in the previous study[5] (Fig 1, available at www.aaojournal.org).

Two patients in each arm did not complete the initial 3-month treatment and were excluded from the analysis. Mean numbers of treatment in ranibizumab arm were 4.4 and 1.4 times in the first and the second years, respectively. The numbers in PDT arm were 1.8 and 0.4 times, respectively. Approximately 20% of the patients switched or discontinued treatment. The main reason for switching treatment was refractoriness to the initial treatment. Three patients in the ranibizumab arm wanted to discontinue or switch to PDT because of treatment burden. Four patients in the PDT arm switched to ranibizumab owing to the development of massive subretinal hemorrhage or type 2 choroidal neovascularization or they received vitrectomy owing to the development of vitreous hemorrhage or vitreomacular traction syndrome. We applied intention-to-treat analysis for these patients and the last observation carried forward approach was used for missing data.

The 24-month visual and anatomic course is shown in Figure 2 (available at www.aaojournal.org). Whereas patients in the ranibizumab arm showed visual gain compared with the baseline at several time points, patients in the PDT arm did not show improvement in vision. Baseline and final logarithm of minimum angle resolution (logMAR) was 0.48±0.27 and 0.40±0.37 in the

ranibizumab arm and 0.57±0.31 and 0.65±0.46 in the PDT arm, respectively. The change in logMAR was significantly different between the 2 groups. ($P = 0.004$) The frequency distribution of the changes in logMAR compared with the baseline is shown in Table 1 (available at www.aaojournal.org). Although several patients in the PDT arm showed improvement in vision, approximately 15% of the patients showed >6 lines of vision loss, which affected the overall outcomes. To confirm the integrity of our results, we also analyzed the difference of the treatment effect using the data of patients who completed the 24-month study (n = 40 in the PDT arm and n = 38 in the ranibizumab arm). In these patients, the baseline and final logMAR were 0.48±0.26 and 0.38±0.39 in the ranibizumab arm and 0.56±0.31 and 0.58±0.43 in the PDT arm, respectively. The change in logMAR was still significantly different between the 2 groups ($P = 0.025$).

Both treatment options succeeded in reducing the retinal thickness despite some fluctuation. The baseline and final central retinal thickness were 366.8±113.6 and 267.8±142.2 μm in the PDT arm ($P < 0.001$) and 418.9±168.6 and 291.2±129.3 μm in the ranibizumab arm ($P < 0.001$), respectively. In contrast with visual changes, the changes in central retinal thickness were not different between the 2 arms ($P = 0.254$).

The results of this study in patients with PCV showed that 3 monthly injections followed by as-needed injections of ranibizumab can achieve better 24-month visual outcomes than PDT. This result was similar to that obtained after 12 months of this trial.[4] Although PDT is sometimes considered superior to anti-VEGF therapy for the treatment of PCV because it can efficiently induce regression of polypoidal lesions, the same may not be implied with respect to the visual outcome. Continuous treatment with anti-VEGF therapy, despite the inferior effect in achieving the regression of polypoidal lesions, can prevent further visual loss in comparison with PDT monotherapy.

Unfortunately, we did not investigate the effect of PDT combined with ranibizumab because we could not recruit a sufficient number of patients to perform a 3-arm comparison, and the effect of combined therapy, the optimal interval of ranibizumab and PDT administration, and the retreatment protocol were not established when we initiated the trial. Because several recent studies report the efficacy of combined therapy, future comparisons of anti-VEGF agents with or without PDT must be performed.

Akio Oishi, MD, PhD[1]
Noriko Miyamoto, MD, PhD[1]
Michiko Mandai, MD, PhD[1]
Shigeru Honda, MD, PhD[2]
Toshiyuki Matsuoka, MD, PhD[3]
Hideyasu Oh, MD, PhD[3]
Mihori Kita, MD, PhD[3]
Tomoko Nagai, MD, PhD[4]
Nobuhiro Bessho, MD, PhD[5]
Mamoru Uenishi, MD, PhD[5]
Yasuo Kurimoto, MD, PhD[1]
Akira Negi, MD, PhD[2]

[1]*Kobe City Medical Center General Hospital, Kobe, Japan;* [2]*Kobe University Graduate School of Medicine, Kobe, Japan;* [3]*Hyogo Prefectural Amagasaki Hospital, Amagasaki, Japan;* [4]*Steel Memorial Hirohata Hospital, Himeji, Japan;* [5]*Mitsubishi Kobe Hospital, Kobe, Japan*

Financial Disclosures: The authors have made the following disclosures: Supported in part by the Japan Society for the Promotion of Science (JSPS), Tokyo, Japan (Grant-in-Aid for Scientific Research, no. 22791706). The funding organization had no role in the design or conduct of this research. Some of the authors (A.O., M.M., S.H., M.K., M.U., Y.K., A.N.) declared payment for lectures from several companies, including Novartis, but the companies had no role in the design or conduct of this research.

References

1. Kokame GT. Polypoidal choroidal vasculopathy-an important diagnosis to make with therapeutic implications. Retina 2012;32:1446–8.
2. Koh AH, Chen LJ, Chen SJ, et al. Polypoidal choroidal vasculopathy: evidence-based guidelines for clinical diagnosis and treatment. Retina 2013;33:686–716.
3. Koh A, Lee WK, Chen LJ, et al. EVEREST STUDY: efficacy and safety of verteporfin photodynamic therapy in combination with ranibizumab or alone versus ranibizumab monotherapy in patients with symptomatic macular polypoidal choroidal vasculopathy. Retina 2012;32:1453–64.
4. Oishi A, Kojima H, Mandai M, et al. Comparison of the effect of ranibizumab and verteporfin for polypoidal choroidal vasculopathy: 12-month LAPTOP study results. Am J Ophthalmol 2013;156:644–51.
5. Fung AE, Lalwani GA, Rosenfeld PJ, et al. An optical coherence tomography-guided, variable dosing regimen with intravitreal ranibizumab (Lucentis) for neovascular age-related macular degeneration. Am J Ophthalmol 2007;143:566–83.

Visual Impairment Owing to Adverse Drug Reaction: Incidence and Routine Monitoring in the United Kingdom

Sight-threatening side effects of medication are rare, but can lead to a considerable individual and societal burden, especially when severe and/or permanent. Because these events are so uncommon, it is challenging to acquire data that clinicians can use to counsel patients or that identify novel potential risks. Currently in the United Kingdom, all serious suspected adverse drug reactions (ADRs) and any drug-related side effect of a new (black triangle) medication[1] are "monitored" through the Medical and Health product Regulatory Agency (MHRA) using the voluntary Yellow Card Scheme[2] to inform an anonymized national database. Classification of ocular ADRs is by eye condition with few categories indicating functional vision. Thus, it is not possible to estimate population incidence of visual impairment owing to ADRs through this source.

We therefore undertook a prospective observational study through the British Ophthalmological Surveillance Unit (BOSU), the long-established national scheme providing anonymized case ascertainment for epidemiologic studies of rare ophthalmic conditions of public health importance.[3] We report on this first systematic national study of incidence of diagnosis of visual impairment owing to ADRs and comparative ascertainment by the MHRA scheme.

Case Definition. Any child or adult newly diagnosed with significant visual loss suspected to be owing to an ADR to any prescribed medication (topical or systemic),[4] including, bilateral or unilateral